Numerical Analysis of Shear Strength Behavior of self-compact reinforced concrete Two-way Bubble Deck Slab with Shear Reinforcement

IOP Conf. Series: Materials Science and Engineering **518** (2019) 022050 doi:10.1088/1757-899X/518/2/022050

Numerical Analysis of Shear Strength Behavior of self-compact reinforced concrete Two-way Bubble Deck Slab with Shear Reinforcement

Ibrahim S. I. Harba[1] and Mais A. Hammed[2]
[1]Assistant Professor, Structural Engineering, Department of Civil Engineering, Al-Nahrain University, Baghdad, Iraq.
[2] Msc. Structural Engineering, Department of Civil Engineering, Al-Nahrain University, Baghdad, Iraq.
E-mail: ibrahim.harba@eng.nahrainuniv.edu.iq, msc.mais1994@gmail.com

Abstract. Bubble Deck is a new construction technology uses hollow plastic balls to eliminate the concrete in the middle part of the solid slab which has a little effect on the performance of the structure. So, this part significantly decreases the self-weight of the structure. Usually, the most critical point in the design of the bubbled slab is the design of a slab-column connection due to the concentration of loads and moments. This paper presents a numerical analysis by ABAQUS/2018 program through using the damage plasticity model to simulate the influence of the cavities due to using the plastic balls on the punching behavior and the effect of strengthening the punching zone by using different shear reinforcement systems on the maximum punching load and deformation capacity. Three slab specimens from the numerical analysis model have been simulated against the experimental results. The calculation of error in the model lies between 4% and 6%. Parametric of study have also been accomplished to realize the effect of the changes in shear reinforcement ratio with bubble slab. It has found that the ultimate strength and deformation capacity have increased when shear reinforcement ratio.

1. Introduction

The slab is one of the most important structural members in creating a space in addition to its largest consumption of the concrete [1]. The first limitation when design a reinforced concrete slab is the span between columns while designing large spans between the columns leads to use of very thick slabs and/ or support beams and increase the dead weight of the structure [2].

Many tries have been prepared for creating biaxial hollow slabs to reduce the weight. Many tries used a fewer weighty material like expanded polystyrene which is laid between the top and bottom of reinforcement, such as waffle slabs/ grid ones. Only waffle slabs have a certain usage in the market, however its use is very limited because of less resistances to fire, local punching and even shear[3]. Bubbled reinforced concrete slab system has been recently introduced in Europe. It was invented by the Danish engineer, Jorgen Breuning in the 1990's [4]. This structural system might optimize the size of vertical members such as columns and walls by reducing the weight of slabs [5].

In this paper, a theoretical analysis to predict the (ultimate load, deflection and crack pattern) of both solid and bubble slab specimens were performed, using a nonlinear finite element (ABAQUS/2018) program based on three reinforced concrete slab tested by Harba and Hammed (2018) [6].

2. Detail of experimental test

2.1. Outline of program

Three slabs were designed to fail in punching shear according to ACI 318M-14 [7] and tested , full details of their dimensions, arrangement of reinforcing steel and dimensions are shown in figure 1 and variables studied are given in table1.

Table 1. Properties of tested slab specimens

Specimen	Type of Specimen	Type of punching shear Reinforcement	Shear reinforcement ratio
SD1	Solid	---------	0
BD1	Bubbled	---------	0
BD3	Bubbled	Closed Stirrups	0.1

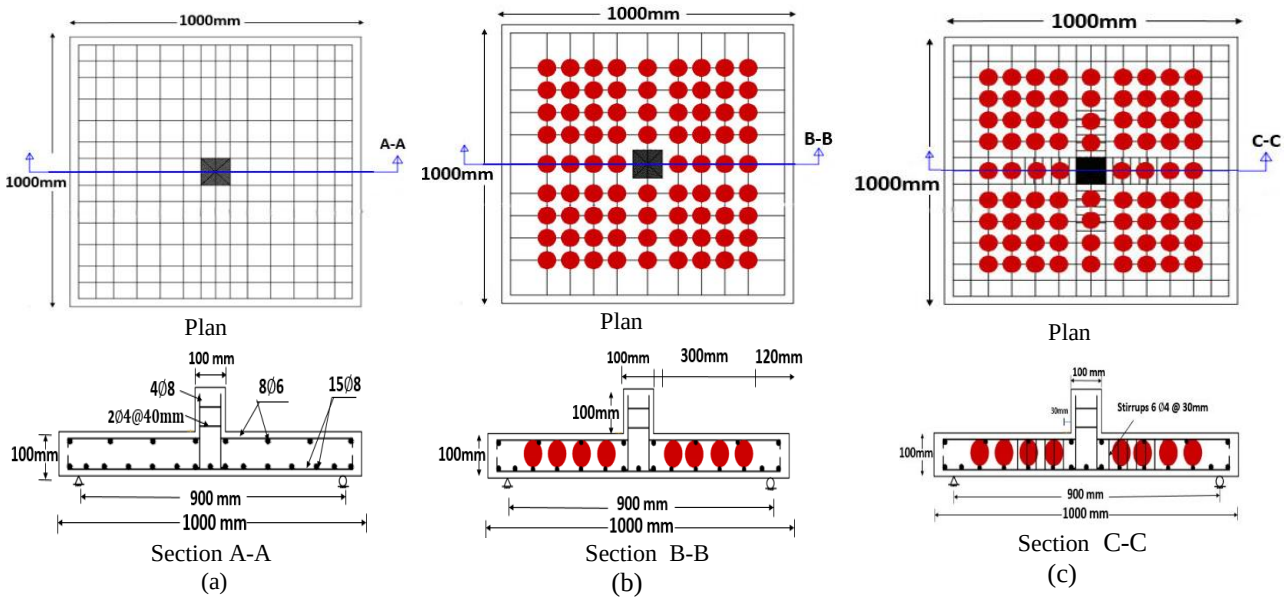

Figure1. Reinforcement details for tested slab specimens (a) SD1 (b) BD1 (c) BD3

2.2. properties of Materials

Self-Compacted Concrete (SCC) used for casting all specimens, it is a type of concrete mix that can flow around overcrowded areas of reinforcement and into tight segments, permit air to escape and avoid segregation without the need for compaction and vibration through the process of pouring. SCC results in durable concrete structures, saves labour and reduction of noise [8].

The design compressive strength of SCC for slab specimens according to (European guidelines, 2005) [9] of (48MPa) cubic strength was used. The proportions of the mixture of concrete are existing in table 2. Reinforcing bars of different size (4, 6 and 8mm) were used in slab specimens. For each size of reinforcement bar, three of the samples were tested under tensile. Table 3 presents the ultimate and yield strength of reinforcing bars. The plastic spheres used in this study with diameters of (60mm) are manufactured in Iraq at (Assajad Factory), from nonporous material that is inert and does not react chemically with the concrete or steel reinforcement and it is made with a small plastic ring which used with the help of tighten wires to fix the bubble with the bottom steel reinforcing mesh [10]. The aim of using recycled material is to restrain using of limited normal resources such as oil and lessen the environmental burden by the cyclical use of resource materials, thus the recycling materials minimize inputs of new resources and limit the burden on the environment and lessen risks on human health.

Table 2. Mix proportions for SCC mix

Cement Kg/m^3	Sand Kg/m^3	Gravel Kg/m^3	Water l/m^3	Superplasticizer l/m^3	Silica Fume Kg/m^3
400	856	767	140	6.5	45

Table 3. characteristics of reinforcing steel bars

Nominal Diameter (mm)	Measured Diameter (mm)	Cross-section Area (mm2)	f_y (MPa)	f_u (MPa)
4	4.105	13.235	466.73	673.51
6	5.86	26.78	532.51	560.64
8	8	50.24	412.82	619.23

2.3. Test method and measurement

All the tested slabs were loaded using a hydraulic jack of 2000 KN capacity. The tested slabs were put in the horizontal position between the jack and a rigid steel frame and adjusted so that the supports, centerline and point load were in their accurate positions as shown in Figure 2. All slabs were tested as a simply supported at all four edges and loaded with a single-point load. Loading was applied slowly in successive increases; the applied load is converted from the testing machine through a central column of dimensions (100x100mm).

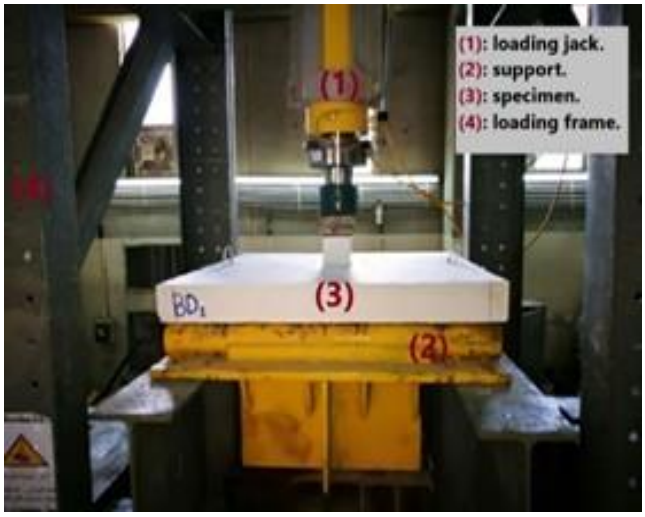

Figure 2. Test Setup

3. Numerical analysis

The concrete damaged plasticity (CDP) is a continuum plasticity depends on the damaged model in which considering the compressive crushing and tensile strength of concrete together as probable modes of failure. CDP is a non-associated and depends on Drucker-Prager hyperbolic function as the plastic potential function. The mode of cracking appears at points in which the maximum principal plastic strain is positive. In tension, the curve of stress-strain of concrete is linear till the ultimate stress. At this ultimate stress, the micro-cracking starts in concrete then after this failure stress, the micro-cracking is noticed macroscopically with a stress-strain softening response that stimulates the localization of strain.

In ABAQUS program, the reinforcement represented by rebars embedded into the concrete. Dowel action and bond slip are indirectly represented through considering tension stiffening to verification the load transfer across the cracks through the reinforcement bars. Tension stiffening is described by using a fracture energy cracking criterion, where the fracture energy is defined as the required energy for opening a unit area of crack. With this criterion, the concrete brittle behavior is considered by a stress-displacement response instead of the usual stress-strain response[11]. Concrete is modelling with 8 node brick (hexahedral) elements with reduced integration (C3D8R) with overall mesh size of 30 mm in a solid slab as shown in figure3 (a) while the use of a rectangular mesh with hexahedron volume is

impossible in bubbled slabs because the bubbled volume has invalid topology for brick meshing. As a result, using the (second order element 10-node quadratic tetrahedral C3D10 with DOF: 3 displacements and 3 rotations) type is necessary to obtain good results as shown in figure 3(b) while the reinforcement bars are modeled by two noded linear truss elements (T3D2). The slab is simply supported along the four sides and loading applied at a stub area of a column with dimensions of (100 mm x 100 mm) as shown in figure 4.

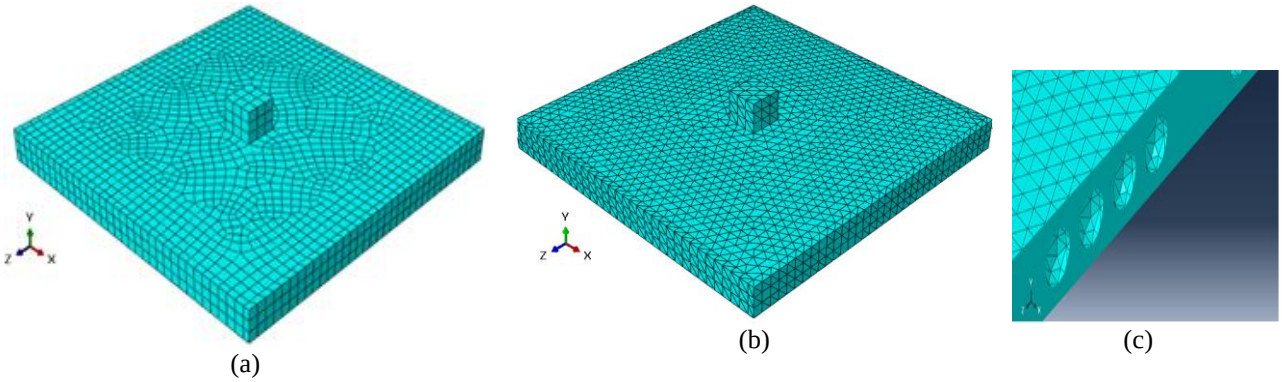

Figure 3. Meshing of Specimens (a) Solid slab (b) bubbled slab (c) voids in bubble slab

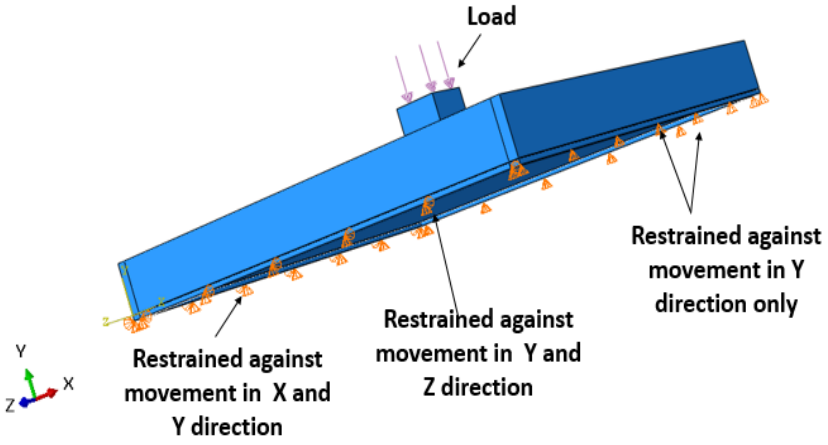

Figure 4. Support conditions simply supported at edges

4. Material modeling

The parameters that needed for describing the concrete properties are: the Poisson's ratio (v), elastic modulus (E_o) were taken as (0.3) and (28588MPa), the tensile and compressive strengths of the tested slabs in addition to complete the non-associated potential flow and the yield of surface, the following data are given:

- Dilation angle (ψ): known as the angle of internal friction of concrete [12], used in this research as 37^o

- Shape factor (Kc): is the coefficient used to determine the form of the deviatory cross-section With a magnitude ranging between (0.64–0.8) used for normal concrete [13], taken as (0.67) according to [14]

- Eccentricity (e): refers to potential flow eccentricity taken as a default value (0.1) [14]

- Stress parameters (σ_{bo}/σ_{co}): it is biaxial compressive yield stress divided by the uniaxial compressive yield stress, for normal concrete the value ranges between 1.10 and 1.16 [15]; in this research sets this parameter equal to 1.16.

- Viscosity Parameter (The magnitude of the viscosity parameter (μ) relates to the increment in time step, (μ) must be about to 15 percent of the increment in the time step so that the solution improved without any change in the results [15])

The compressive strength behavior of concrete in the damaged plasticity model defined as tabular stress-strain relationship regarding to section (3.1.5) in Eurocode 2 which has a behavior of linear elastic until (40 percent) of compressive strength of concrete and then the behavior of non-linear of concrete begins and continues until the ultimate compressive strain of the concrete material [16].

While the uniaxial relation stress–strain of rebars was modeled in elastic properties with Poisson's ratio (v) and Young's modulus (E_S) of which have a values of 0.3 and 200,000 MPa respectively and the plastic behavior was defined by yield stress of each bars.

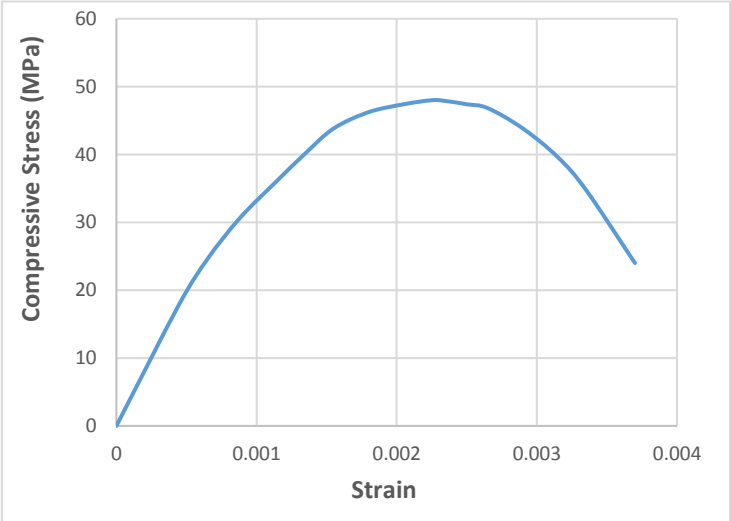

Figure 5. The compressive stress-strain behavior of concrete according to Eurocode 2 [16]

5. Results of verification slab specimens

5.1. Load-deflection Relationships of the tested slab Specimens

The experimental and numerical results of the failure load capacity and ultimate deflection are summarized in table 4 for tested slab specimens. The FEA of load-deflection relationships for tested specimens are shown in figure 6 while figure 6 shows the deflected shapes due to applied loads.

It can be noted that there is an agreement between the experimental and the numerical results nearby (104%) of failure load (Pu), and around (93%) for deflection at ultimate load (Δu) and these percentages are viewed accepted and reasonable.

The ultimate loads that achieved from the experimental results are greater than numerical analysis by about (2~6) %. It is useful to note that the failure in FEA indicates to the failure of one element in the structure while the failure in the experimental work indicates to failure in the all elements of the structure. Thus, smaller deflections are observed in the FEA than experimental results.

Table 4. Numerical and experimental results

Slab	Experiment (E)		Numerical (N)		Load Correction Factor PuN/ PuE	Deflection Correction Factor ΔuN/ ΔuE
	Pu (kN)	Δu (mm)	Pu (kN)	Δu (mm)		
SD1	189.8	12.34	193.74	11.13	1.021	0.902
BD1	127	13.63	135	12.8	1.063	0.939
BD3	139.7	12.43	145	12.08	1.038	0.972
AVARAGE					1.041	0.938

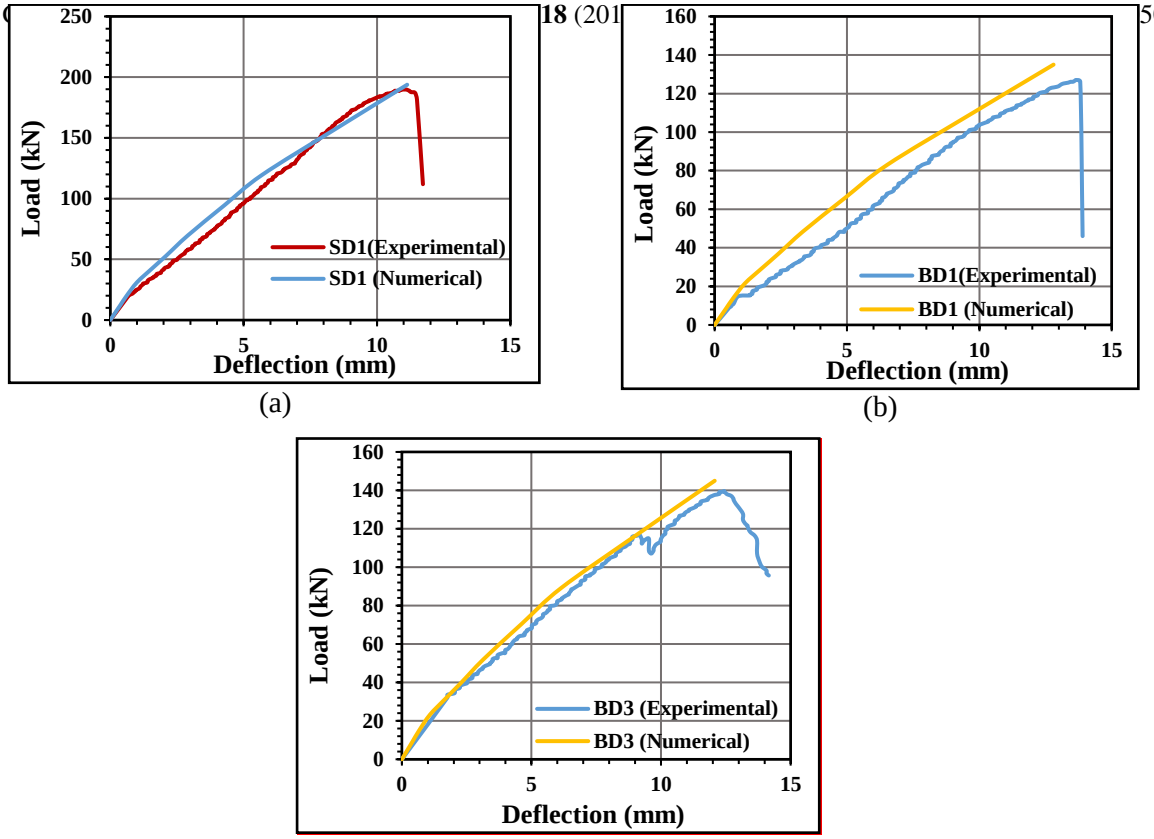

Figure 6. Load- Deflection Response for slab specimen (a) SD1 (b) BD1 (c) BD3

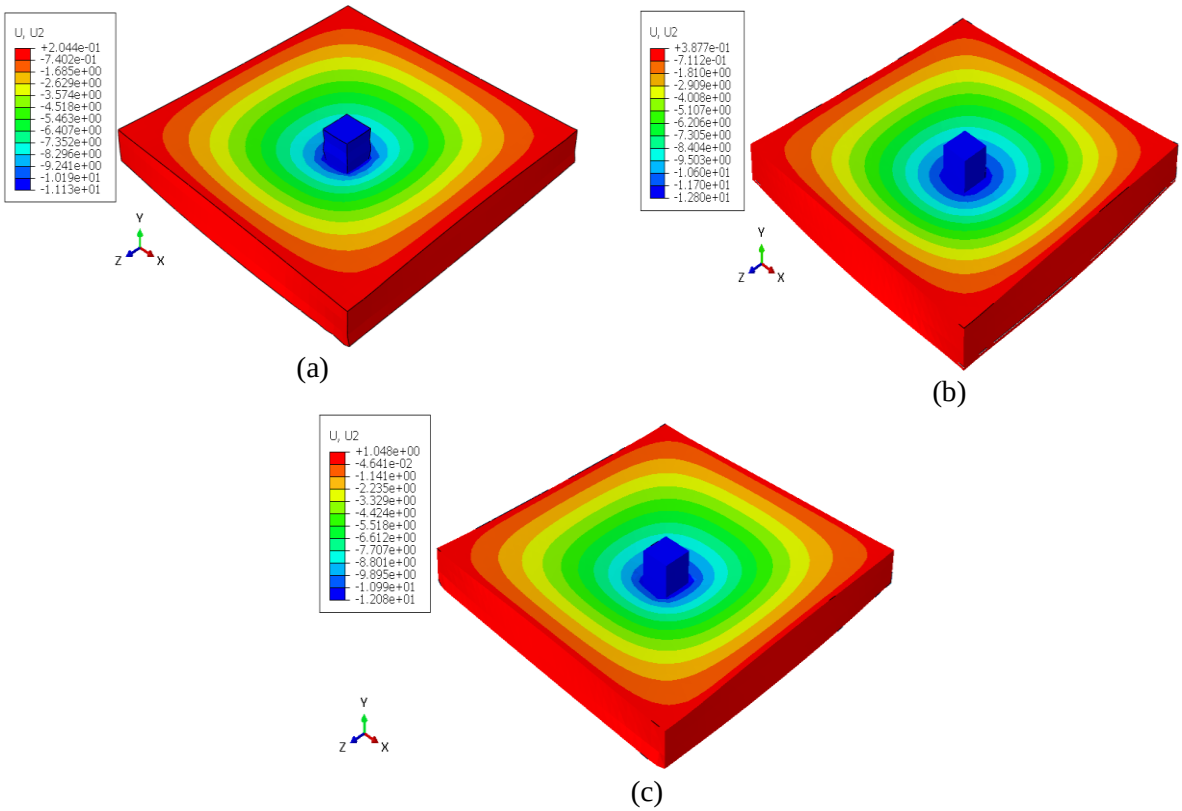

Figure 7. Deflected Shape for slab specimen (a)SD1 (b) BD1 (c) BD3

5.2. Crack Patterns of slab specimens

A comparison between the crack patterns mode from the FEA results with that obtained from the experimental test are shown in figures 8, 9 and 10.

Based upon the observed cracking patterns, it can be noticed that there is a reasonable agreement between the FEA and the experimental response for the modeled concrete beams crack patterns.

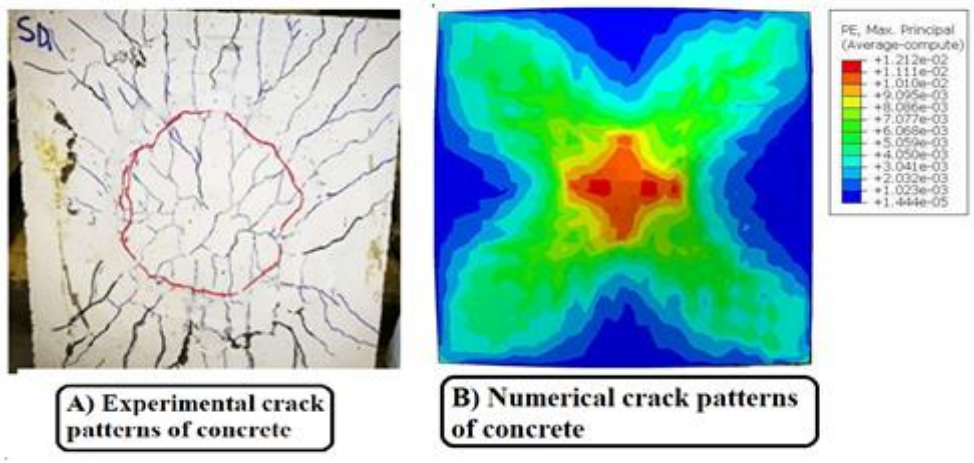

Figure 8. Crack pattern mode on tension surface for specimen SD1

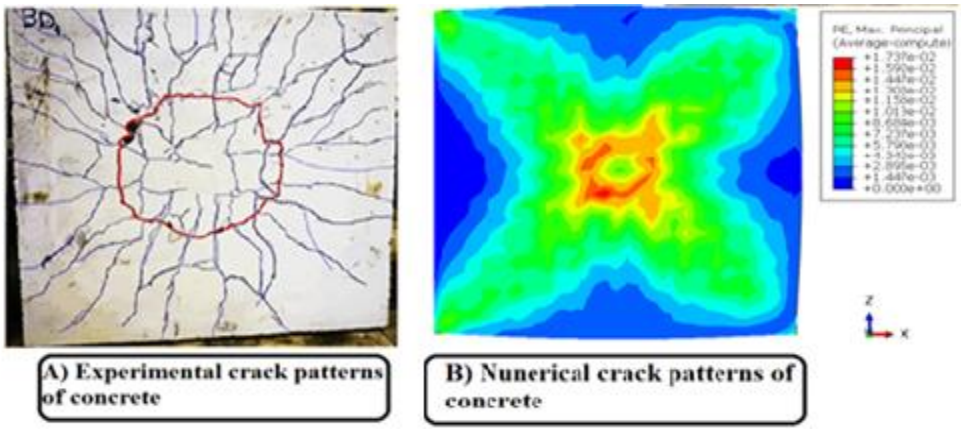

Figure 9. Crack pattern mode on tension surface for specimen BD1

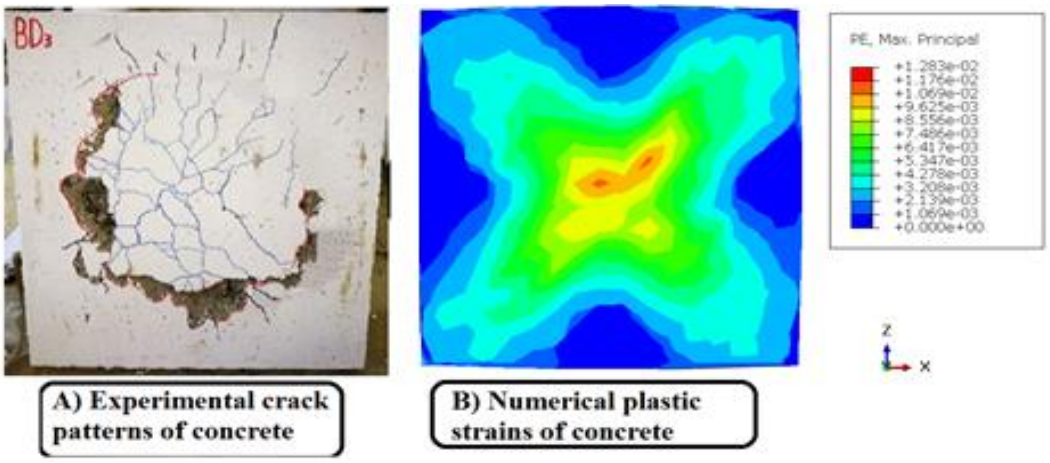

Figure 10. Crack pattern mode on tension surface for specimen BD3

6. Parametric study

The acceptability and verification of the results among the FEA and experimental work prepared additional parameters to study the effect of changing shear reinforcement ratio and shear reinforcement systems on the behavior of bubble deck slab specimens. Three bubbled slab specimens similar to the tested specimens mentioned in section 2.1 in dimensions and reinforcement details with study parameters listed in table 5. Figure 11 show the reinforcement details of the numerical specimens BDI-S8, BDI-Ml8 and BDO-Mm3.

Table 5. Study parameters proposed by ABAQUS

Slab Specimen	Type of specimen	Position of Bubbles with respect to critical zone[a]	Type of punching shear Reinforcement
BDI-S8	Bubbled	Inside	Closed stirrups Ø 8
BDI-Ml8	Bubbled	Inside	Multiple-leg stirrups Ø 8
BDO-Mm3	Bubbled	Out side	Middle-Mesh (Three layers)

[a]According to the ACI318M-14, the critical perimeter is assumed at 0.5 of effective depth of slab (d) from the perimeter of the loaded area.

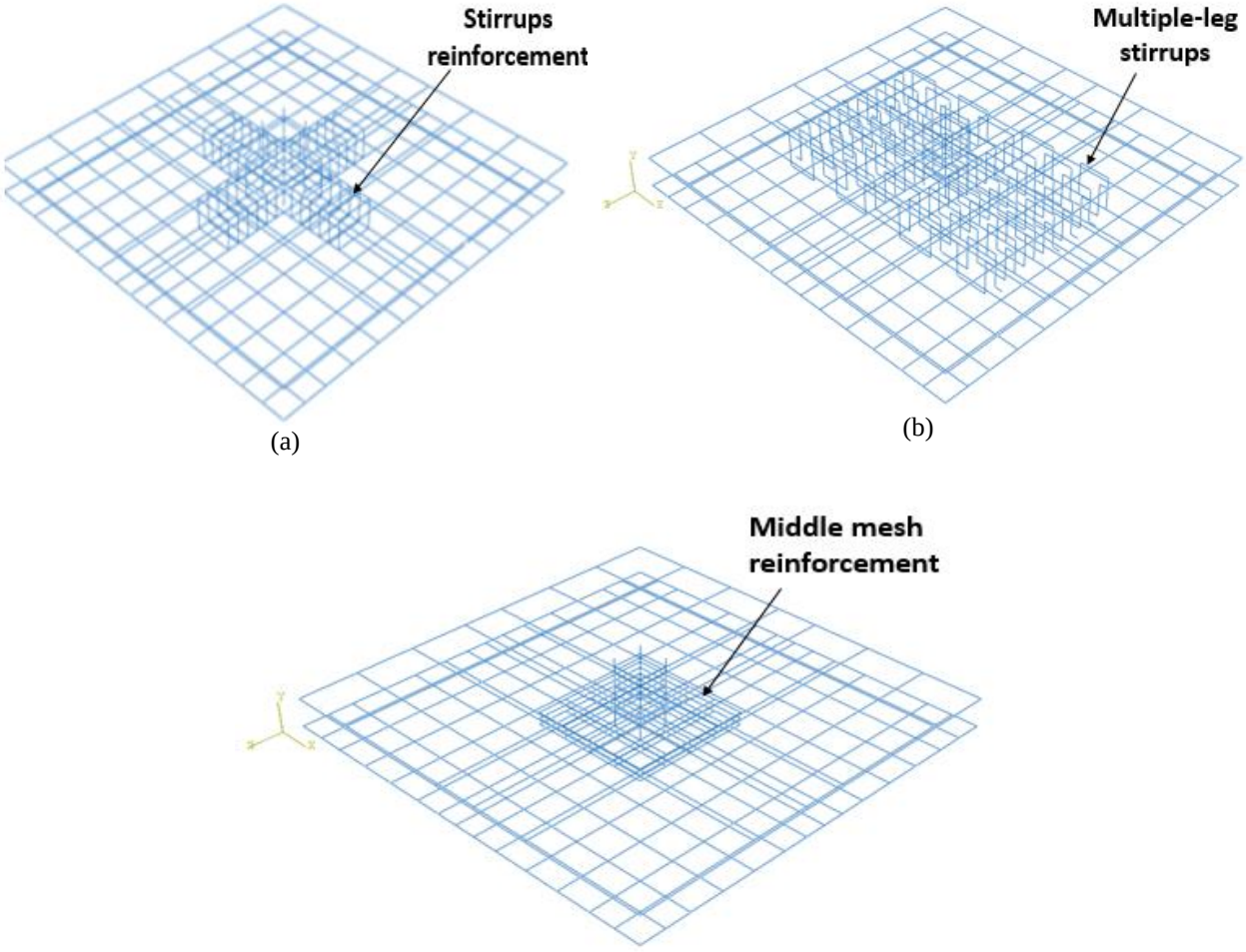

Figure 11. Reinforcement details for numerical specimens (a) BDI-S8 (b) BDI-Ml8 (c) BDO-Mm3

7. Numerical Results

7.1. Load-deflection relationships of the numerical slab specimens

The load versus mid-span deflection for finite element models BDI-S8, BDI-Ml8 and BDO-Mm3 are presented in figures. 12, 13 and 14. The comparisons of their results for mid-span deflection and failure load with experimental reference slabs results BD1, and BD2 (details mentioned in section 2.1) are presented in the table 6. In addition, the deflected profiles of the FEM are shown in the figures. 15, 16 and 17.

Finite element models BDI-S8 and BDI-Ml8 that reinforced with closed stirrups and multiple leg stirrups with reinforcement ratio of (0.397% and 1.586%) exhibited an increase in the strength capacity equal to 38% and 96% and a reduction in the ultimate deflection about 41% and 21% compared with the control specimen (BD1). And in specimen BDO-Mm3 that reinforced with middle mesh reinforcement and reinforcement ratio of 3.101% show an increase in the strength capacity equal to 34% and reduction in ultimate deflection by about 34% compared with the control specimen (BD1).

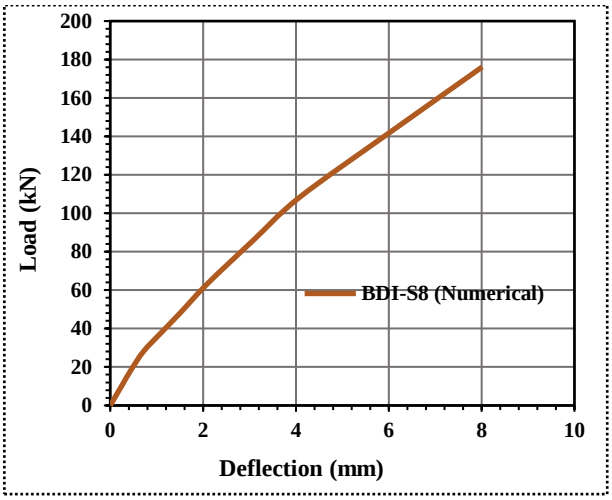

Figure12. Load- Deflection Response for Slab BDI-S8

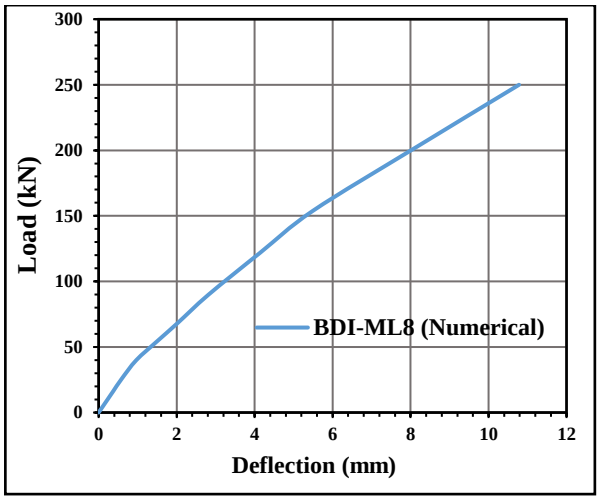

Figure13. Load- Deflection Response for Slab BDI-Ml8

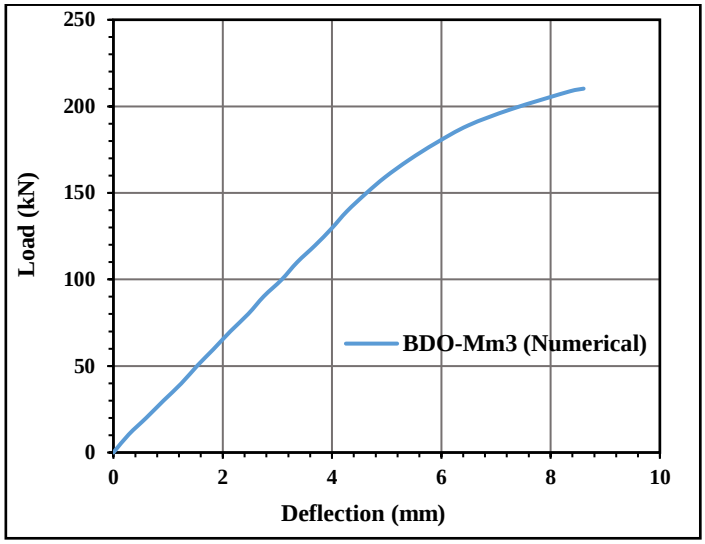

Figure 14. Load- Deflection Response for Slab BDO-Mm3

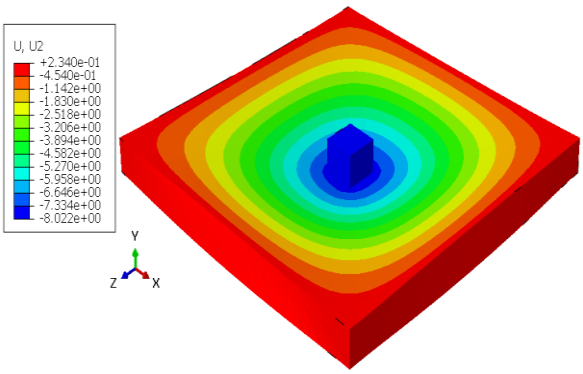

Figure 15. Vertical Displacement along Longitudinal Direction of BDI-S8

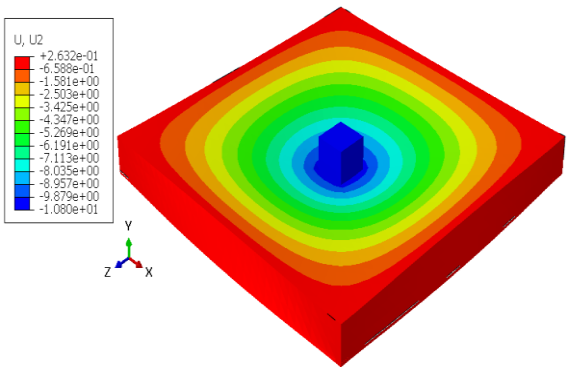

Figure 16. Vertical Displacement along Longitudinal Direction of BDI-Ml8

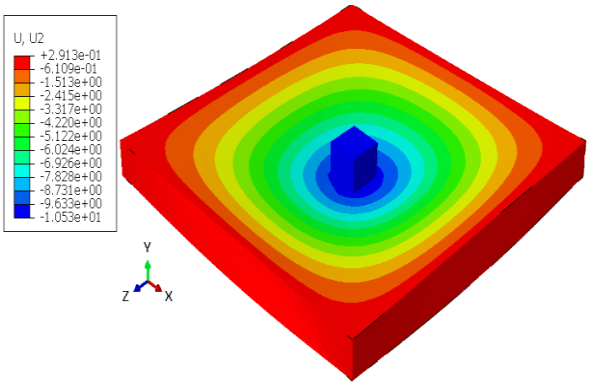

Figure 17. Vertical Displacement along Longitudinal Direction of BDO-Mm3

Table 6. Comparison of Ultimate Load - Displacement between FEA models with Exp. Specimen (BD1) and (BD2)

Numerical Slab Specimens	**Ultimate load $P_{u\text{-}FEA}$ (KN)**	**$P_{u\text{-}FEA}$/ $P_{u\text{-}EXP.\ (reference)}$**	**Δu (mm)**	**Δu_{FEA}/ $\Delta u_{EXP.\ (reference)}$**
BD1 (Reference)	127	…..	13.63	……
BDI-S8	176.1	1.39	7.99	0.586
BDI-Ml8	250	1.97	10.78	0.791
BD2 (Reference)	156.55	…….	13.22	……
BDO-Mm3	210.2	1.34	8.6	0.651

7.2. Crack Patterns of slab specimens

The concrete damage plasticity model (CDPM) presents the crack directions through supposing that the direction of crack is comparable with the path of the maximum principal plastic strain. So, the crack development in the FEA simulations can be tracked through the principal equivalent tensile strains in the concrete. The cracking is shown at the bottom view of the slab in specimens BDI-S8 and BDI-Ml8, figures18 and 19.

Firstly, the crack mode in specimens (BDI-S8 and BDI-Ml8) occurs with tangentially at the maximum bending moment zone adjacent to the column and then extends radially to edges of the slab whenever the load increases while specimen BDI-Ml8 gradually failed in a flexural mode, figure 20.

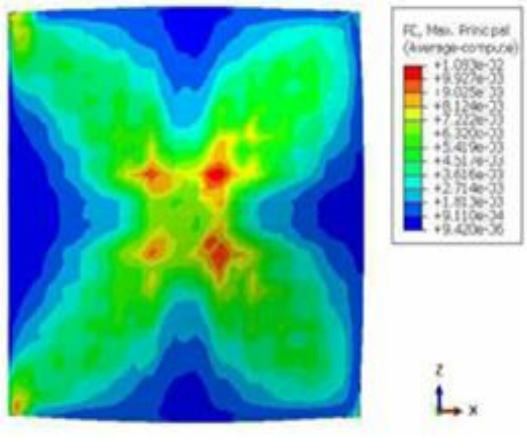

Figure 18. Crack pattern mode on tension surface for specimen BDI-S8

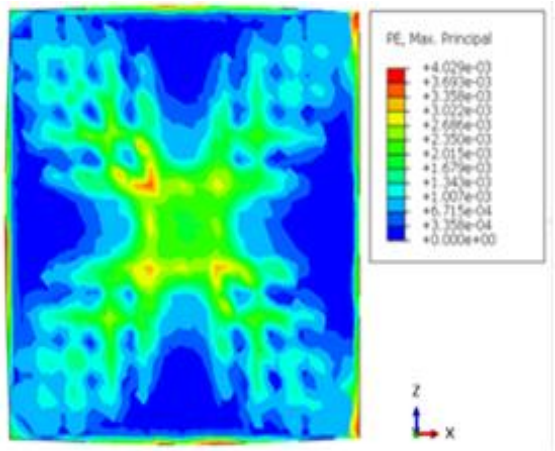

Figure 19. Crack pattern mode on tension surface for specimen BDI-Ml8

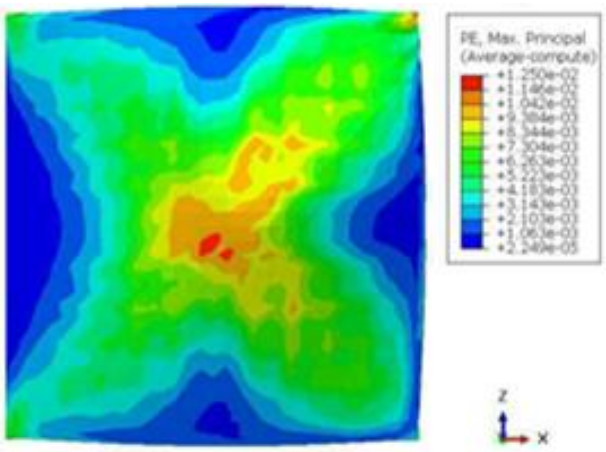

Figure 20. Crack pattern mode on tension surface for specimen BDO-Mm3

8. Conclusion

Based on the numerical results, certain conclusions can be derived as follows:

1. Modeling and analyzing the tested specimens by using ABAQUS/2018 program, it notes that there is a good agreement between the results of the numerical models and the experimental performance of the tested specimens.
2. The finite element load-deflection curves are somewhat stiffer than the experimental responses for the tested slabs.
3. The ultimate loads from the experimental results are lower than the ultimate loads of the finite element analyses.
4. The ultimate load of the Bubble Deck slab obtained from the finite element analysis is lower than the solid slab.
5. The mode of crack patterns at the ultimate loads that is obtained from the numerical models agree well with the modes of the failure observed in the experimental slabs.
6. Using punching shear reinforcement in bubble slab is effective due to its contribution in changing the failure modes, which is very important characteristics for determining the safety of the structures.
7. Shear reinforcement ratio shows a significant part for enhancing the punching shear strength and the deformation capacity of the slab specimens and converts the failure mode from brittle to flexural ductile failure when increase the punching shear reinforcement.

References

[1] Chung J H, Choi H K, Lee S C and Choi C S 2011 Flexural Capacities of Two-Way Hollow Slab with Donut Type Void. *Proceeding of annual conference of the architectural institute of Korea*.
[2] Midkiff C J 2013 Plastic Voided Slab Systems: Applications and Design *Msc. Thesis Kansas* State University. Manhattan, USA.
[3] Joseph A V 2016 Structural Behaviour of Bubble Deck Slab *M-Tech Seminar Report*.
[4] Fuchs A C 2009 BubbleDeck Floor System-An Innovative Sustainable Floor System. *BubbleDeck Netherlands BV, AD Leiden, the Netherlands*.
[5] Schellenbach-Held S E and Pfeffer K 1998 BubbleDeck-New Ways in Concrete Building. *Technical University Darmstadt's, Germany* 110–140.
[6] Harba I S I and Hammed M A 2018 Shear behavior of self compacted reinforced concrete two way bubble slabs *International Journal of Civil Engineering and Technology (IJCIET)* **9** 1117–1127.
[7] ACI 318 2014 Building code requirements for structural concrete and commentary, Farmington Hills, MI: American Concrete Institute (ACI).
[8] Gencel O, Brostow W, Datashvili T and Thedford M 2011 Workability and mechanical performance of steel fiber-reinforced self-compacting concrete with fly ash *Composite interfaces* **18** 169–184.
[9] EFNARC 2005 The European guidelines for self compacting concrete specification, production and use *Self-compacting Concr*.
[10] Oukaili N K and Husain L F 2016 Punching shear strength of bubbledecks under eccentric loads. *Proceeding of Second International Conference on Science, Engineering and Environment* Osaka City Japan pp.222-227.
[11] Genikomsou A and Polak M A 2017 Finite element simulation of concrete slabs with various placement and amount of shear bolts *Procedia engineering* **193** 313–320.
[12] Kmiecik P and Kamiński M 2011 Modelling of reinforced concrete structures and composite structures with concrete strength degradation taken into consideration *Archives of civil and mechanical engineering* **11** 623–636.
[13] Jankowiak T and Lodygowski T 2005 Identification of parameters of concrete damage plasticity constitutive model. Foundations of civil and environmental engineering **6** 53–69.
[14] Abaqus Theory Manual. Abaqus User's Man. Version 6.8, n.d.
[15] Lee J and Fenves G L 1998 Plastic-damage model for cyclic loading of concrete structures *Journal of engineering mechanics* **124** 892–900.
[16] EN B S 2004 Eurocode 2: Design of concrete structures Part 1-1–General rules and rules for buildings (including NA) *London: British Standards Institution*.